Shaping the luminescence spectrum of nanophosphor and improved chromaticity of the red color via polymorphism of the lattice

A. I. Kostyukov[1], V. N. Snytnikov[1,2], Vl. N. Snytnikov[1], A. V. Ishchenko[1,2], M.S. Molokeev[3,5,6], A.S. Krylov[3], and A.S. Aleksandrovsky[3,4]

[1]Boreskov Institute of Catalysis, Lavrentieva Ave. 5, 630090, Novosibirsk, Russia

[2]Novosibirsk State University, Pirogova Str. 2, 630090, Novosibirsk, Russia

[3] Kirensky Institute of Physics Federal Research Center KSC SB RAS, Krasnoyarsk 660036, Russia

[4] Department of Photonics and Laser Technology, Siberian Federal University, Krasnoyarsk 660041, Russia

[5] Siberian Federal University, Krasnoyarsk, 660041, Russia

[6] Department of Physics, Far Eastern State Transport University, Khabarovsk, 680021, Russia

ABSTRACT: Europium doped Y_2O_3 nanoparticles obtained via cw laser evaporation are shown to crystallize in monoclinic symmetry class (C2/m space group). The size of nanoparticles established via HRTEM coincides with coherent scattering region established by XRD. Luminescence spectrum in the vicinity of ultranarrow transition demonstrates three peaks consistent with three inequivalent positions of Eu^{3+} ion in monoclinic Y_2O_3 lattice. Hypersensitive transition dominates in the spectrum, admitting the lack of inversion symmetry at C_s sites occupied by Eu^{3+}. The spectrum of hypersensitive transition is expanded to the red part of spectrum due intense transitions terminating at higher-lying components of crystal-field-split $^7F_2$ energy level. Obtaining chromaticity coordinates (0.669, 0.331) is possible using red phosphor based on monoclinic Y_2O_3:Eu^{3+}. Current investigation revealed unique possibility of crystal field shaping of Eu^{3+} luminescence spectrum in a polymorph of Y_2O_3 which will result in high color purity and meets technology needs in a number of wLED applications.

■ Introduction

Investigations of new red phosphors are presently extremely abundant area of materials research. Prominent progress is achieved with Eu^{2+} ion in different hosts including nitrides (see e.g. [1,2] and references therein) and oxides [3-5] via crystal field engineering of the spectral shift of f-d emission of this ion. The choice of the host crystal structure and variation of chemical content of some already investigated hosts for Eu^{2+} ions allows wide tuning of color properties of divalent europium phosphors as well as resulting solid state lighting sources based on them. Red phosphors based on trivalent europium were extensively investigated in the past, and commercial phosphorswere created, one of them being Y_2O_3:Eu^{3+} with cubic crystal structure. Spectral properties of trivalent europium luminescence are controllable by the choice of host, too, but to the much smaller extent than those of divalent europium. In the particular, chromaticity coordinates of commercial cubic Y_2O_3: Eu^{3+} are (0.65, 0.35) that is not well suitable for some applications.

Chromaticity of phosphors based on trivalent europium is determined by the distribution of intensities between luminescent bands originating from higher-lying $^5D_0$ energy level and terminating at low-lying ^7F_J (J=0…6) states. Hypersensitive transition to $^7F_2$ state typically is dominating in efficient phosphors since its maximum oscillator strength induced by crystal field is favorable to combat radiationless losses. Distribution of intensities of transitions between individual crystal-field-split subcomponents within this band varies from the host to host, and typically the maximum of emission lies between 610 and 620 nm. (For several recent examples of shaping the spectra of trivalent europium see e. g. [6](612 and 616 nm), [7](611 nm), [8] (613.9 nm).Attractive results in tailoring the luminescence spectrum of trivalent europium were obtained in $Ba_2Gd_2Si_4O_{13}$[9] where chromaticity coordinates (0.66, 0.34) were reported.

Oxides of rare earth elements, including yttrium, can crystallize in several crystalline structures, including cubic (*Ia*3), hexagonal ($P\bar{3}m1$) and monoclinic (*C*2/*m*) [10]. Monoclinic polymorphs can be obtained under the high pressure but the transition is irreversible. Properties of europium in these crystalline structures are not studied up to date. The aim of the present study is to

obtain nanoparticles of europium doped monoclinic polymorph of Y_2O_3 (m-Y_2O_3:Eu^{3+}) and to investigate its spectral properties.

■ Experimental techniques

Synthesis of europium doped m-Y_2O_3 nanoparticles. Y_2O_3:Eu nanoparticles were obtained by laser vaporization of Y_2O_3:Eu(5mol.%Eu_2O_3, $T_{cal.}$=850 °C/4 h) ceramic targets irradiated by a cw CO_2 laser (radiation wavelength 10.6 μm, generation power up to 110 W on one TEM_{00} transverse mode, output beam diameter 8 mm, divergence in the far-field region 3×10^{-3} rad) with subsequent condensation of vapor in a Ar (99.99%) buffer gas flow in a vaporization chamber. Laser power on the target surface was 103 W (the power density 5.5×10^4 W/cm^2). A detailed description of a setup used for the synthesis of nanomaterials can be found in [11-12].

Characterization. Elemental chemical analysis of the samples was made using X-ray fluorescence spectroscopy (XRF) on an ARL – Advant'x analyzer with the Rh anode of the X-ray tube. The morphology of the synthesized samples was characterized by high-resolution transmission electron microscopy (HRTEM) on a JEM-2010 electron microscope at accelerating voltage 200 kV and resolution 1.4 Å. Samples were deposited on a copper grid by dispersing a solid phase suspension in alcohol using an ultrasonic disperser.

The powder diffraction data of Y_2O_3:Eu and of pure Y_2O_3 initial cubic compound for Rietveld analysis were collected at room temperature with a Bruker D8 ADVANCE powder diffractometer (Cu-Kα radiation) and linear VANTEC detector. The step size of 2θ was 0.016°, and the counting time was 2 s per step.High-resolution luminescence spectra were obtained using Horiba JobinYvon T64000 spectrometer and GaN laser excitation source at the central wavelength 408 nm.

■ RESULTS AND DISCUSSION

HRTEM and XRD results. As shown by the elemental analysis performed by XRF, after vaporization of the 5 mol. % Eu_2O_3/Y_2O_3 target and subsequent condensation of vapor, europium enters the composition of the produced Y_2O_3 nanoparticles with the close concentration.

Figure 1 displays HRTEM images of the nanosized$Y_2O_3:Eu^{3+}$ sample.TEM images of $Y_2O_3:Eu^{3+}$ sample demonstrate that particles have a spherically symmetric shape and are represented by nanocrystallites with the average size d_{av}=11.7±6.3 nm. HRTEM images of the sample show interplanar distances that can be attributed mainly to monoclinicY_2O_3:Eu (PDF# 87-2361).

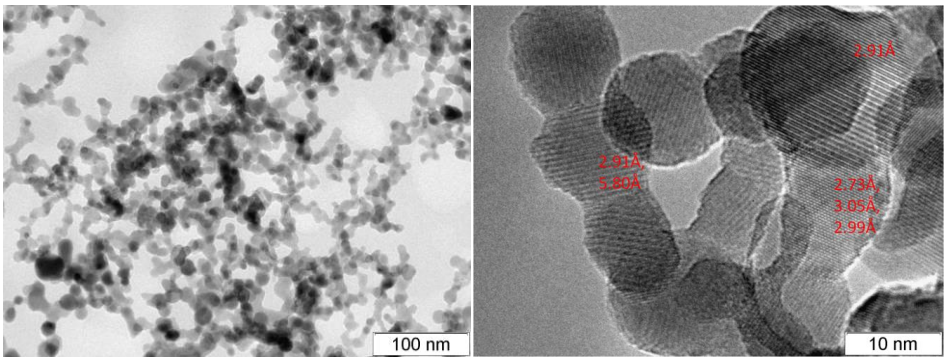

Figure 1.HRTEM images of Y_2O_3:Eu sample with interplanar spacing.

All peaks of powder pattern were indexed by monoclinic cell (*C*2/*m*) with parameters close to Sm_2O_3[13]. Therefore this structure was taken as starting model for Rietveld refinement which was performed using TOPAS 4.2 [14]. Sm ions at all three inequivalent sites were changed to Y ions in the starting model before refinement. In order to reduce number of refined parameters, only one thermal parameter was refined for all O atoms. Refinement was stable and gave low *R*-factors (Table 1, Figure 2a). Coordinates of atoms and main bond lengths are in Table 2 and Table 3 respectively. Estimated nanocrystal size from refinement was equal to 9.3(3) nm, in good agreement with HRTEM results. Initial compound was fitted by well-known cubic Ia-3 phase (Table 1, Figure 2b). Possible content of cubic polymorph in the nanocrystalline sample can be estimated to be below 5%.

The crystallographic data are deposited in Cambridge Crystallographic Data Centre (CCDC #??????). The data can be downloaded from the site (www.ccdc.cam.ac.uk/data_request/cif).

Table 1. Main parameters of processing and refinement of the m-Y_2O_3:Eu and c-Y_2O_3samples

Compound	Y_2O_3:Eu	Y_2O_3 initial
Sp.Gr.	*C*2/*c*	*Ia-3*
a, Å	13.964 (2)	10.823 (2)
b, Å	3.5009 (6)	–
c, Å	8.6308 (17)	–
β, º	100.185 (9)	–
V, Å^3	415.30 (13)	1267.8 (7)
Z	6	16
2*θ*-interval, º	5-140	5-100
R_{wp}, %	3.71	3.01
R_p, %	2.88	2.18
R_{exp}, %	2.53	2.03
χ^2	1.46	1.48
R_B, %	0.74	0.84

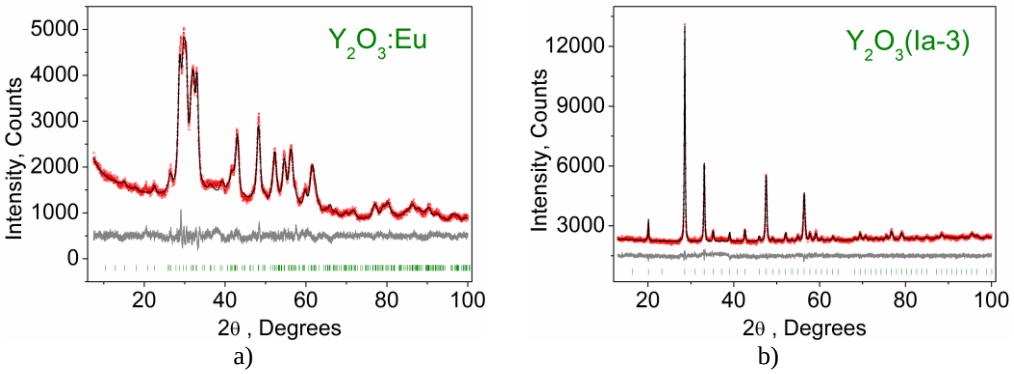

Figure 2. Difference Rietveld plot of: a) nanoparticles of m-Y_2O_3:Eu; b) cubic Y_2O_3.

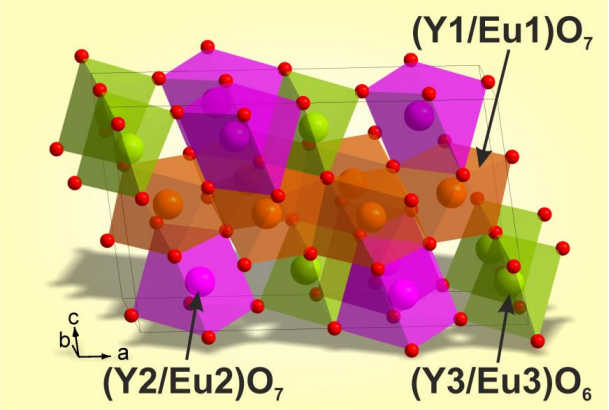

Figure 3. Crystal structure of monoclinic Y_2O_3:Eu with three inequivalent positions for Y/Eu.

Table 2. Fractional atomic coordinates and isotropic displacement parameters (Å^2) of Y_2O_3:Eu

Atom	Wyck off site	Local symmetry	*x*	*y*	*z*	B_{iso}
Y1	4*i*	*m*	0.1337 (4)	0.5	0.4876 (5)	0.5 (7)
Y2	4*i*	*m*	0.1887 (4)	0.5	0.1427 (6)	0.7 (7)
Y3	4*i*	*m*	0.4642 (5)	0.5	0.1864 (7)	0.3 (7)
O1	4*i*	*m*	0.115 (2)	0	0.333 (2)	1.2 (8)
O3	4*i*	*m*	0.2740 (19)	0.5	0.365 (4)	1.2 (8)
O4	4*i*	*m*	0.465 (2)	0	0.333 (3)	1.2 (8)
O5	2*b*	2/*m*	0	0.5	0	1.2 (8)
O2	4*i*	*m*	0.327 (2)	0.5	0.029 (3)	1.2 (8)

Table 3. Main bond lengths (Å) of Y_2O_3:Eu

Y1—O1	2.188 (11)	Y2—O5	2.704 (5)
Y1—O3	2.39 (2)	Y2—O2	2.32 (2)
Y1—O3^{i}	2.40 (2)	Y2—O2^{iii}	2.279 (17)
Y1—O4^{ii}	2.49 (2)	Y3—O1^{iv}	2.26 (2)
Y1—O4^{i}	2.25 (3)	Y3—O4	2.159 (15)
Y2—O1	2.724 (16)	Y3—O5^{iv}	2.487 (4)
Y2—O3	2.07 (3)	Y3—O2	2.14 (3)

Symmetry codes: (i) -*x*+1/2, *y*+1/2, -*z*+1; (ii) *x*-1/2, *y*+1/2, *z*; (iii) -*x*+1/2, *y*+1/2, -*z*; (iv) *x*+1/2, *y*+1/2, *z*

Luminescence. Fig. 4 presents overall high-resolution luminescence spectrum of m-Y_2O_3:Eu^{3+}(red lime) in comparison with that of reference crystal α-$Eu_2(MoO_4)_3$[15] (blue line).

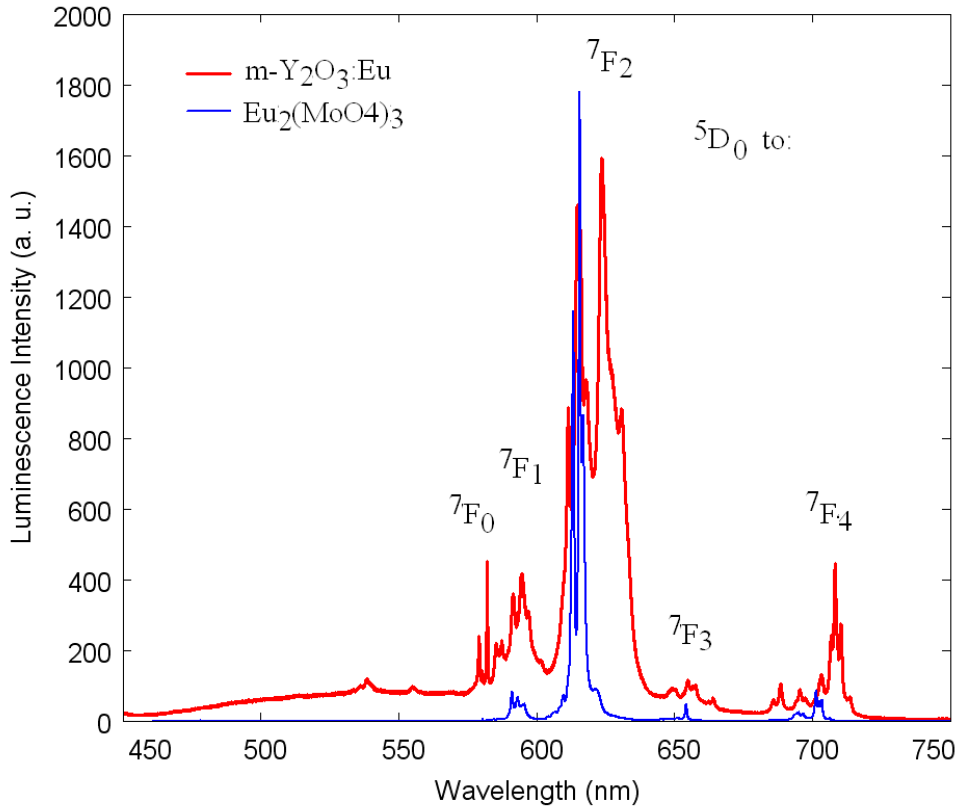

Figure 4. Overall luminescence spectrum of m-Y_2O_3:Eu excited at 408 nm (red) in comparison with the luminescence of α-$Eu_2(MoO_4)_3$ (blue).

Crystal-field-induced electric dipole band $^5D_0$ - $^7F_2$ dominates over magnetic dipole band $^5D_0$ - $^7F_1$ in this spectrum, indicating sufficient degree of inversion symmetry violation in the local environment of trivalent europium ion. The spectral region of ultranarrow transition of trivalent europium ion is presented in Fig.5 in more detail.

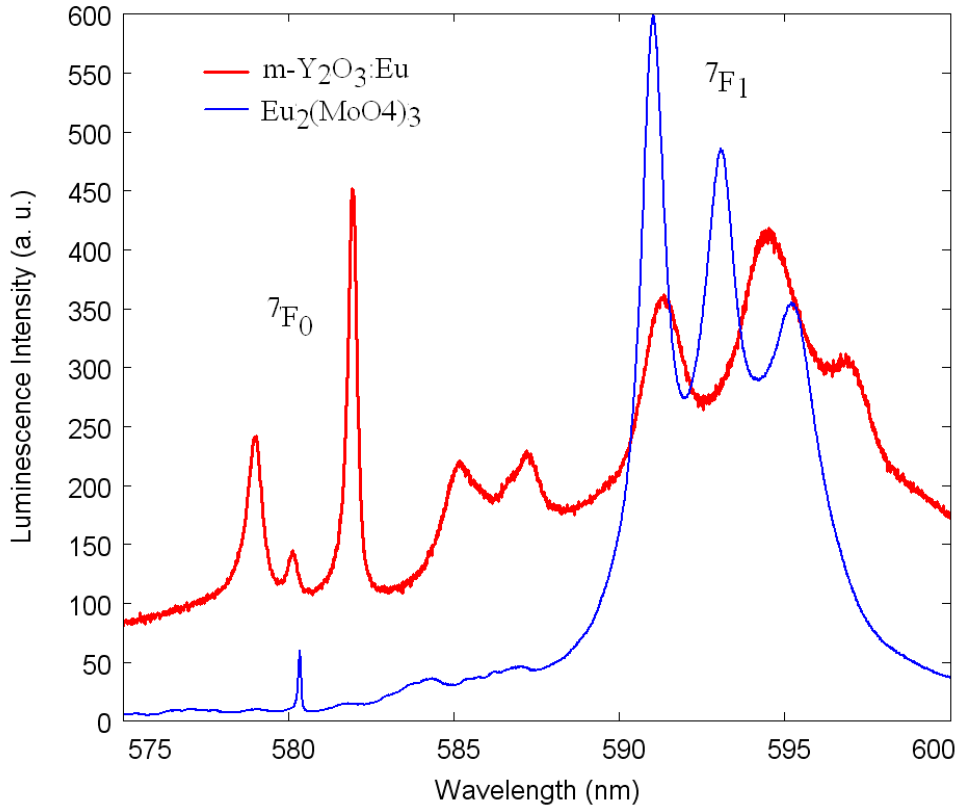

Figure 5. Luminescence spectrum in the vicinity of ultranarrow transition for m-Y_2O_3:Eu excited at 408 nm (red) in comparison with the luminescence of α-$Eu_2(MoO_4)_3$ (blue).

In contrast to the spectrum of reference crystal with its single inequivalent position of europium ion, local symmetry of which being C_1, the spectrum of m-Y_2O_3:Eu^{3+} exhibits three peaks in the region of $^5D_0$ - $^7F_0$ transition that is consistent with three inequivalent positions for Y in crystal structure of monoclinic Y_2O_3 polymorph, the local symmetry of all three being C_s. The maxima of these $^5D_0$ - $^7F_0$ transitions are positioned at 578.973, 580.103 and 581.909 nm; therefore, energies of $^5D_0$ states are 17272, 17238.3 and 17184.8 cm^{-1}.The narrowest of $^5D_0$ - $^7F_0$ lines must be associated with octahedral site of Y within m-Y_2O_3 structure while two others must be ascribed to sites with monocapped trigonal prism local environment. The width of peak at 581.909 nm equals to 11.2 cm^{-1}, being 3.5 times wider than ultranarrow peak in α-$Eu_2(MoO_4)_3$(3.1 cm^{-1}). This broadening must be ascribed to size broadening of luminescence lines observed in nanoparticles.

The peak at 581.909 nm exceeds the peaks of neighboring $^5D_0$ - $^7F_1$ transition that means rather high degree of violation of mirror symmetry at its site.

The spectral structure of $^5D_0$ - $^7F_2$ band is shown in Fig. 6 in more detail.

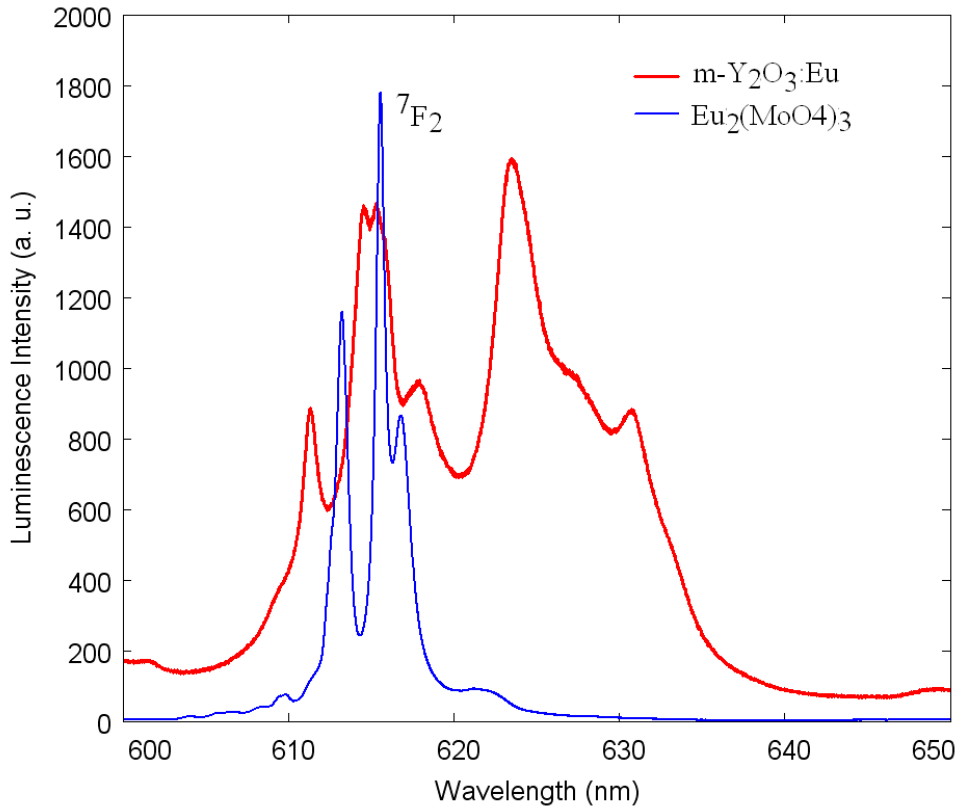

Figure 6. Luminescence band terminating at $^7F_2$ energy level for m-Y_2O_3:Eu excited at 408 nm (red) in comparison with that of α-$Eu_2(MoO_4)_3$ (blue).

The maxima of this band are positioned at 615 and 623 nm, the latter being of even higher height, and additional longer-wavelength peaks exist with wings protruding up to 635 nm. This part of spectrum is present in cubic $Y_2O_3:Eu^{3+}$ but its amplitude in c-$Y_2O_3:Eu^{3+}$ is less than in m-$Y_2O_3:Eu^{3+}$. Additional subbands in the spectral range from 620 to 635 nm within $^5D_0$ - $^7F_2$ luminescent band of m-Y_2O_3: Eu^{3+} must be ascribed to the transitions from $^5D_0$ in three inequivalent sites to highest components of crystal-field-split $^7F_2$ manifold.

In addition to emission originating from $^5D_0$ state, weak emission from $^5D_1$ to $^7F_{0,1,2}$ is detectable in the spectrum of m-Y_2O_3: Eu^{3+} presented in Fig.4. One may notice that narrow Eu^{3+} emission bands are observed above the background that is represented by broad band from 460 to 720 nm with the maximum approximately at 600 nm. This band must be assigned to the presence of divalent europium in m-Y_2O_3 nanoparticles. The excitation maximum is expected to lie in the UV, and observed emission is the long-wavelength wing of the whole possible emission band of divalent europium. Nevertheless, this contribution strongly affects the chromaticity coordinates of m-Y_2O_3:Eu nanophosphor. Calculation over the whole emission range of m-Y_2O_3: Eu results in (0.582 0.381) chromaticity coordinates, while calculation over emission range of Eu^{3+} ion results in (0.669, 0.331) ones. The latter values are desired for some applications, for instance they are very close to the standard recommended by NTSC. Therefore, complete stabilization of Eu^{3+} valence state in m-Y_2O_3 is promising for creation of new standard source of red color, while optimization of Eu^{3+}/Eu^{2+} content and of the excitation wavelength gives is the potential way for creation of white phosphor.

■ Conclusion

Europium doped Y_2O_3 nanoparticles were obtained via cw laser evaporation. XRD analysis shows that laser evaporation enables crystallization of Y_2O_3 in the crystal structure belonging to monoclinic symmetry class (C2/m space group). HRTEM evidences formation of spherical nanoparticles with the diameter of order of 10 nm and with good crystallinity. Luminescence spectrum in the vicinity of ultranarrow transition demonstrates three peaks consistent with three inequivalent positions of Eu^{3+} ion in monoclinic Y_2O_3 lattice. Hypersensitive transition dominates in the spectrum admitting the lack of inversion symmetry at C_s sites occupied by Eu^{3+}. The spectrum of hypersensitive transition is broadened to the red part of spectrum due intense transitions terminating at higher-lying components of crystal-field-split $_7F_2$ energy level. Obtaining chromaticity coordinates (0.669, 0.331) is possible using red phosphor based on monoclinic Y_2O_3:Eu^{3+}. We believe that further developments of the technology of monoclinic Y_2O_3:Eu will result in the efficient phosphor with improved chromaticity that will be useful in a number of high-quality wLED sources.

■Acknowledgment

This work is financially supported by the Russian Foundation for Basic Research № **19-32-60027**.

■ References

1. Mu-Huai Fang, Sebastian Mahlik, Agata Lazarowska, Marek Grinberg, Maxim S. Molokeev, Hwo-Shuenn Sheu, Jyh-Fu Lee, Ru-Shi Liu. Structural Evolution and Effect of the Neighboring Cation on the Photoluminescence of $Sr(LiAl_3)_{1-x}(SiMg_3)_xN_4:Eu^{2+}$ Phosphors. Angewandte Chemie International Edition, 58(23), (2019), pp.7767-7772.
2. Chun Che Lin, Yi-Ting Tsai, Hannah E. Johnston, Mu-Huai Fang, Fengjiao Yu, Wuzong Zhou, Pamela Whitfield, Ye Li, Jing Wang, Ru-Shi Liu, and J. Paul Attfield, Enhanced Photoluminescence Emission and Thermal Stability from Introduced Cation Disorder in Phosphors. J. Am. Chem. Soc. 2017, 139, 11766−11770.
3. Ming Zhao, Yayun Zhou, Maxim S. Molokeev, Qinyuan Zhang, Quanlin Liu, Zhiguo Xia. Discovery of New Narrow-Band Phosphors with the UCr_4C_4-Related Type Structure by Alkali Cation Effect. Advanced Optical Materials, 7 (2019), pp.180163 1-9.
4. Ming Zhao, Hongxu Liao, Maxim S. Molokeev, Yayun Zhou, Qinyuan Zhang, Quanlin Liu, Zhiguo Xia. Emerging ultra-narrow-band cyan-emitting phosphor for white LEDs with enhanced color rendition. Light: Science & Applications, 8, 38, (2019), pp.1-9.
5. 4.Hongxu Liao, Ming Zhao, Maxim S. Molokeev, Quanlin Liu, and Zhiguo Xia. Learning from a Mineral Structure toward an Ultra-Narrow-Band Blue-Emitting Silicate Phosphor $RbNa_3(Li_3SiO_4)_4:Eu^{2+}$. Angewandte Chemie, 57(36) (2018) pp.11728-11731.
6. Yuriy G. Denisenko, Victor V. Atuchin, Maxim S. Molokeev, Aleksandr S. Aleksandrovsky, Alexander S. Krylov, Aleksandr S. Oreshonkov, Svetlana S. Volkova, Oleg V. Andreev. Structure, Thermal Stability, and Spectroscopic Properties of Triclinic Double Sulfate $AgEu(SO_4)_2$ with Isolated SO_4 Groups. Inorganic Chemistry, (2018)57№2113279-13288.

7. Atuchin, V. V.; Subanakov, A. K.; Aleksandrovsky, A. S.; Bazarov, B. G.; Bazarova, J. G.; Gavrilova, T. A.; Krylov, A. S.; Molokeev, M. S.; Oreshonkov, A. S.; Stefanovich, S. Yu.Structural and Spectroscopic Properties of Noncentrosymmetric Self-activated Borate $Rb_3EuB_6O_{12}$ with B_5O_{10} Units.Mater.Des.2018, 140, 488−494.
8. 7.VictorV. Atuchin,AleksandrS. Aleksandrovsky,BairG. Bazarov,JibzemaG. Bazarova, OlgaD. Chimitova,YuriyG. Denisenko, TatyanaA. Gavrilova, AlexanderS. Krylov, EugeneA. Maximovskiy, MaximS. Molokeev,AleksandrS. Oreshonkov, AlexeyM. Pugachev,NikolayV. Surovtsev. Exploration of structural, vibrational and spectroscopic properties of self-activated orthorhombic double molybdate RbEu $(MoO_4)_2$ with isolated MoO_4 units. J. AlloysCmpnd. 2019, 785, 692− 697.
9. 8. HaiGuo, Hao Zhang, RongFei Wei, MengDiZheng, LiHong Zhang. Preparation, structural and luminescent properties of $Ba_2Gd_2Si_4O_{13}:Eu^{3+}$ for white LEDs.Opt. Express. 2011. 19, No. S2 A201 – A206.
10. 9. Henry R. Hoekstra, Karl A. Gingerich.High-Pressure B-Type Polymorphs of Some Rare-Earth Sesquioxides.Science, 1964. 14, 1163-1164.
11. 10. V.N. Snytnikov, Vl.N. Snytnikov, D.A. Dubov, V. I. Zaikovskii, A.S. Ivanova, V.O. Stoyanovskii, V. N. Parmon. Production of nanomaterials by vaporizing ceramic targets irradiated by a moderate-power continuous-wave CO_2 laser, Journal of Applied Mechanics and Technical Physics 48 (2) (2007) 292–302.
12. 11. A. Kostyukov, M. Baronskiy, A. Rastorguev, V. Snytnikov, Vl. Snytnikov, A. Zhuzhgov and A. Ishchenko, Photoluminescence of Cr^{3+} in nanostructured Al_2O_3 synthesized by evaporation using a continuous wave CO_2-laser. RSC Advances 6(3) (2016) 2072 – 2078.
13. 12. Schleid, T., & Meyer, G..Single crystals of rare earth oxides from reducing halide melts. Journal of the Less Common Metals, 149 (1989)73-80.
14. 13. Bruker AXS TOPAS V4: General profile and structure analysis software for powder diffraction data. – User's Manual. Bruker AXS, Karlsruhe, Germany. 2008.

Код поля изменен

15. 14. Atuchin, V. V.; Aleksandrovsky, A. S.; Chimitova, O. D.; Gavrilova, T. A.; Krylov, A. S.; Molokeev, M. S.; Oreshonkov, A. S.; Bazarov, B. G.; Bazarova, J. G. Synthesis and Spectroscopic Properties of Monoclinic α-Eu2(MoO4)3. J. Phys. Chem. C 2014, 118, 15404− 15411.

Supporting information

Shaping the luminescence spectrum of nanophosphor and improved chromaticity of the red color via polymorphism of the lattice

A. I. Kostyukov[1], V. N. Snytnikov[1,2], Vl. N. Snytnikov[1], A. V. Ishchenko[1,2], M.S. Molokeev[3,5,6], A.S. Krylov[3], and A.S. Aleksandrovsky[3,4]

[1]Boreskov Institute of Catalysis, Lavrentieva Ave. 5, 630090, Novosibirsk, Russia

[2]Novosibirsk State University, Pirogova Str. 2, 630090, Novosibirsk, Russia

[3] Kirensky Institute of Physics Federal Research Center KSC SB RAS, Krasnoyarsk 660036, Russia

[4] Department of Photonics and Laser Technology, Siberian Federal University, Krasnoyarsk 660041, Russia

[5] Siberian Federal University, Krasnoyarsk, 660041, Russia

[6] Department of Physics, Far Eastern State Transport University, Khabarovsk, 680021, Russia